ce/papers Proceedings in civil engineering

Ernst & Sohn A Wiley Brand

ORIGINAL ARTICLE

ibausil
F. A. Finger-Institut für Baustoffkunde
Bauhaus-Universität Weimar

Effect of cement composition and the storage conditions on the morphology of ASR products in concrete

Miriam E. Krüger[1] | Anne Heisig[1] | Detlef Heinz[2] | Alisa Machner[1]

Correspondence

Dr.-Ing. Anne Heisig
Technical University of Munich
TUM School of Engineering and Design
Department of Materials Engineering
cbm Centre for Building Materials
Professorship for Mineral Construction Materials
Franz-Langinger-Str. 10
81245 München
Email: anne.heisig@tum.de

[1] TUM, Professorship for Mineral Construction Materials, Munich, Germany
[2] TUM, Professorship for Mineral Engineering, Munich, Germany

Abstract

Under natural conditions, the alkali silica reaction (ASR) is a slow degradation process in concrete. Therefore, accelerated laboratory test methods are used to estimate the alkali-reactivity of aggregates and concrete performance regarding a damaging ASR. In this study, concrete cubes were stored in a fog chamber at 40 °C/100% RH and at outdoor conditions in Munich climate for up to 9 years. Opaline sandstone/flint (25 vol.%) was used as reactive aggregate. 15 wt.% of OPC was replaced by fly ash and compared with the reference mix with 100 wt.% OPC. The cracks widths of the cubes were measured regularly. To investigate the effect of accelerating test conditions on the morphology of reaction products, the concrete microstructure, pore solution composition and ARS products formed under accelerated and field conditions were investigated. The present study shows that accelerated test methods consider only partial aspects of the complex mechanisms of ASR in concretes containing pozzolanic fly ash. Storage conditions have a direct effect on the morphology of the ASR products, the porosity and the pore solution composition of the concrete. When testing blended binders under accelerating conditions, opposing mechanisms are achieved and the chemical and physical processes can be changed significantly.

Keywords

Alkali silica reaction, ASR product, fly ash, accelerating conditions, outdoor storage, pore solution analysis, mercury intrusion porosimetry, SEM-EDX

1 Introduction

Alkali-silica reaction (ASR) is a well-known chemical deterioration mechanism in concrete leading to substantial maintenance costs each year. In order to test the performance of a concrete with regard to damaging ASR, various test procedures at accelerating conditions are used to speed up the reaction mechanism (e.g. exposure temperatures of 40 °C or 60 °C) [1–3]. Due to the accelerating conditions, reaction kinetics are altered and can therefore, beside other effects on porosity and hydration products of the binders, affect the formation, structure and composition of the ASR product, the so-called alkali-silica gel (ASR gel). After the ASR gel is formed it can partly transform to a crystalline ASR product, which shows similarities to the mineral shlykovite [4; 5]. However, the crystalline ASR product is not expected to cause damage in concrete [4; 5]. The ASR gel on the other hand, can build-up considerable swelling pressure on concrete, while absorbing water, which leads to structural damage. The composition of the ASR gel is variable and depends on several factors, such as the chemical environmental condition, and can alter over time [6].

The alteration of the ASR gel composition may in turn have a direct effect on the swelling capacity and therefore the damage potential in the concrete. The swelling pressure evolves due to the adsorption of water and electrostatically repulsion of dissociated negatively charged silicate layers [7]. Dependent on the degree of crosslinking of the silicate framework, the incorporation of the water amount is limited, therefore swelling is expected to change [8].

It is well-known that the use of supplementary cementitious materials (SCMs) can reduce the risk for ASR by reducing the alkalinity of the pore solution, [9; 10] changing porosity [11–13] and binder phase composition (especially C-S-H and C-A-S-H phases) [10; 14; 15] as well as affecting the composition of the ASR gel [16]. Up to now, the effect of storage conditions on morphology and composition of ASR products was rarely investigated. Therefore, the present study considers laboratory and outdoor storage conditions for concretes with an ASR potential and the effect of fly ash (FA) on the morphology of ASR products.

https://doi.org/10.1002/cepa.2943

2 Materials and methods

2.1 Concrete composition

In this study, coarse aggregates (gravel containing opaline sandstone, EIII-O-OF in grading B/C 8), which is no longer available for a general use in commercial concretes, were used as reactive aggregates (Table 1) to achieve a remarkable amount of ASR products. Due to the pessimum effect of this reactive aggregate, 25 wt.% of the gravel with opaline sandstone was mixed with a crushed inert diabas and an unreactive gravel (EI) to reach B/C 16 grading (Table 2). To study the effect of an aluminous pozzolanic SCM, fly ash (FA) was mixed with a CEM I 32.5 R (OPC).

Table 1 Mineralogical composition of the gravel with opaline sandstone (EIII-O-OF), as determined by XRD with Rietveld analysis in wt.%.

Amorphous	Quartz	Orthoclas	Plagioclas	Muscovite	Calcite
26	39	9	15	4	7

The concretes were prepared with 500 kg/m³ binder (100 wt.% OPC and 75 wt.% OPC+15 wt.% FA) at a w/b ratio of 0.5. The cement was replaced by weight with FA (k-value = 1) keeping the w/b ratio constant. The equivalent alkali content of the OPC was 1.0 wt.%. The FA with an equivalent alkali content of 3.5 wt.%, an Al_2O_3 content of 26.2 wt.% and an amorphous content of 72.6 wt.% used fulfilled the specifications of DIN EN 450-1 [17]. The cement was replaced by 15 wt.% FA, which is an insufficient amount to inhibit damaging ASR for reactive aggregates but was used to study the composition and morphology of the formed ASR products. Additionally, FA was selected as another source for aluminum in the binder composition. Since, ASR products formed in concretes containing metakaolin and other calcined clays in the binder showed differences in composition and thus presumably in their swelling behavior [18].

Table 2 Concrete composition (100 wt.% OPC, 75 wt.% OPC and 15 wt.% FA).

		OPC	OPC-15FA
Cement	[kg/m³]	500	425
Fly ash	[kg/m³]	0	75
	[wt.%]	0	15
w/b ratio		0.5	
0/2 Sand	[vol.%]	52	
2/8 EIII-O-OF		25	
2/8 Diabas		5	
8/16 EI		18	

Concrete cubes (300 mm) were prepared and exposed to 40 °C and 100 % RH in the fog chamber and to the outdoor climate in Munich (cfb: temperate oceanic climate according to the Köppen-Geiger classification [19], Figure 1).

The climate in Munich, where some of the concrete cubes were exposed to (outdoor storage), is generally warm and temperate. Munich has a significant amount of rainfall during the year. The average temperature in Munich is 8.8 °C with a precitpitation of around 1000 mm per year. The maximum temperature with 37.0 °C in summer was reached 2015 [20]. It has to be noticed that surface temperatures of concrete due to solar radiation can be assumed to be around 7 °C higher [21]. During the winter an average of 73 days with temperatures under 0 °C are to be expected [22] with a freezing exposure to the concrete samples in outdoor storage.

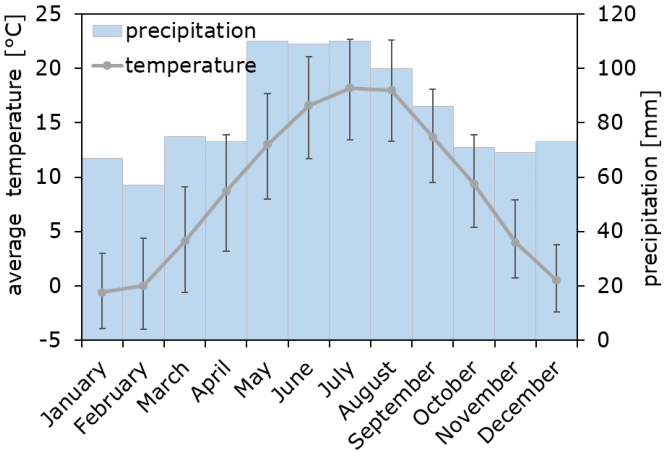

Figure 1 Average climate data per month in Munich (Köppen-Geiger classification: cfb) from 1991-2021. Dataset: European Centre for Medium-Range Weather Forecasts (ECMWF) [23].

2.2 Methods

The samples were exposed to 40 °C and 100 % RH in a fog chamber according to the ASR guideline of the German committee of reinforced concrete [1] and the outdoor storage, respectively. Crack width measurements of the cubes were carried out regularly on samples stored in the fog chamber and in the outdoor storage for up to 9 years.

Additionally, to exhibit the effect of 15 wt.% FA, pastes were prepared with a w/b ratio of 0.5 and stored in sealed flasks to avoid leaching and carbonation. After 24 h hardening in an overhead shaker at 20 °C, the flasks were cured for 1, 28 and 91 days at 20 °C and 9 month at 40 °C.

Pore size distributions were determined on pastes and concrete samples by mercury intrusion porosimetry (MIP) using an AutoPore IV 9500 mercury pressure porosimeter from Micrometrics Instrument Corporation. The contact angle of the mercury was assumed to be 130° and the surface tension to be 485 dyn/cm. Binder and concrete were broken to fragments (20 mm). Since the pore size distribution was measured partially on concrete samples with an undefined proportion of aggregate, a quantitative comparison of the total porosity was not considered. To discuss the results, the proportion of pores measured was normalized to 100 % of each concrete. However, the trend of the pore size distributions remains unaffected, which makes a qualitative comparison possible. The threshold diameter between capillary and gel pores was set to 0.02 µm.

Pore solutions were expressed from paste specimens and the chemical composition of the pore solution was analysed using inductively-coupled plasma optical emission spectroscopy (ICP-OES) using an Avio 500 ICP-OES from Perkin Elmer. The hydroxyl ion concentration was determined by titration.

After 4.5 and 9 years, thin sections were prepared on concrete samples with 15 wt.% fly ash (OPC-15FA) in the binder and with 100 wt.% OPC (OPC) and examined by polarized light microscopy.

Scanning electron microscopy (SEM)-based automated mineralogy was performed on four thin sections at the Minerals and Materials Characterizations (MiMaC) EM laboratory located at the Department of Geoscience and Petroleum, NTNU Norway. For the investigations, the OPC concrete after 4.5 and 9 years at outdoor storage and after 9 years in the fog chamber were choosen. To investigate the long-term effect of FA on the ASR product composition, the concrete sample OPC-15FA was also tested after 9 years in the outdoor storage. The MiMaC-EM laboratory runs a ZEISS Sigma 300VP field emission SEM that is equipped with 2 Bruker Xflash 6|60 129 eV energy dispersive X-ray spectroscopy (EDS) detectors, a backscatter electron (BSE) and secondary electron (SE) detectors, as well as the ZEISS Mineralogic software for automated quantitative mineralogical (AQM) analysis.

For each of these analyzed areas, mineral and BSE maps are simultaneously produced, as well as data tables for quantitative modal mineralogy (bulk mineralogy) and pixel data. Due to the amorphous nature of the ASR gels and abundance of only micron-sized grains, a small step size of 1 µm was chosen to detect the variations in composition in the phases of interest. Element heat maps (EHM) were used for visualizing intensities of elements of interest. To avoid unnecessary measuring of epoxy, thresholding and other arithmetic image processing scripts were applied.

3 Results and discussion

3.1 Measurements of crack widths

Figure 2 shows the crack width development of the concrete samples stored in the fog chamber and in the outdoor storage measured for up to 9 years. In both storage regimes the sample OPC exhibit larger crack widths compared to the sample OPC-15FA. For concretes stored in the fog chamber it can be expected that cracks are solely caused by ASR and the formation of swelling ASR gels. While cracks of the samples exposed to natural weathering are also widened by frost attack during the winter period. Additionally, these samples are exposed to varying temperatures and humidites during the year (Figure 1).

According to the threshold value (crack width below 0.2 mm after 9 months) for fog chamber storage [1], the concrete OPC-15FA pass. However, after one to two years, samples of the same composition but stored outdoors start to crack with a maximum crack width of 0.75 mm after 9 years. Therefore, to assess the alkali sensitivity of these concretes solely on the basis of the fog chamber storage results would lead to an incorrect assessment. The enhanced and constant temperatures in the fog chamber may lead to an accelerated pozzolanic reaction of the fly ash. This might affect the capillary porosity or/and causes a shift in the chemical equilibrium in the concrete pore solution, which will be discussed in the following chapter (3.2).

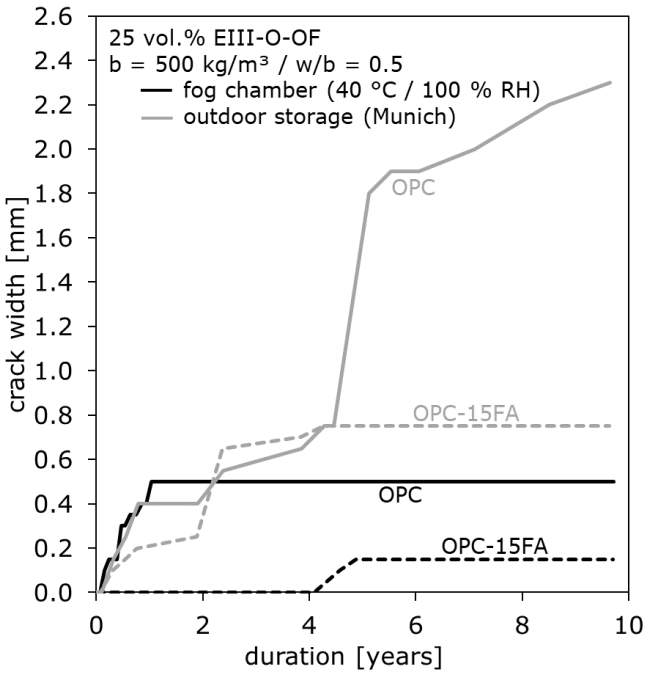

Figure 2 Development of crack width in concrete cubes (300 mm) stored in the fog chamber (over 40 °C/100 % RH) and outdoor storage (Munich climate: cfb).

3.2 Effect on porosity and pore solution composition

3.2.1 Mercury intrusion porosity

MIP measurements were performed on pastes and concretes containing OPC and OPC-15FA. The results show similarities between the different paste and concrete samples (Figure 3).

As expected, the proportion of capillary pores in all samples decreased significantly between 1 and 28 days due to hydration. After 1 day of hydration the portion of capillary pores in samples OPC-15FA is somewhat higher than in the samples OPC. However, capillary porosity decreases more significantly between 28 and 91 days in the samples containing fly ash, which can be explained by the beginning pozzolanic reaction.

Another series of samples was pre-cured for 1 day at 20 °C and subsequently stored in the fog chamber at 40 °C for 9 months. The capillary porosity of the OPC concrete decreases with 22 % between 1 day and 9 months, while in the concrete OPC-15FA, the capillary porosity decreases of around 33 wt.% (not shown here). This difference is due to an acceleration of the pozzolanic reaction under higher temperatures, as also published by Schmidt et al. [24]. This indicates that even for 15 wt.% fly ash in the binder the pore structure shifts to lower capillary pores due to the pozzolanic reaction. This densification decreases the ion transport processes, which limit the formation of ARS products and may lead to an overevaluation of the fly ash concrete assessed in the fog chamber.

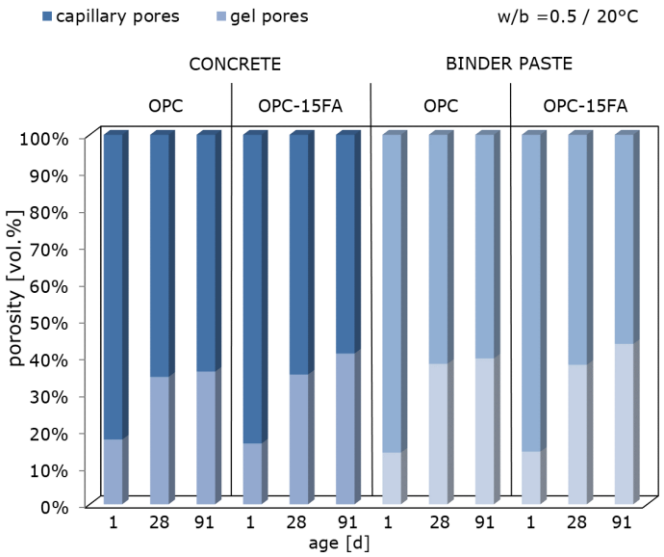

Figure 3 Portion of capillary and gel porosity in concrete and paste samples after 1, 28 and 91 days at 20 °C measured by MIP.

3.2.2 Pore solution analysis

For pore solution analysis, solely paste samples were investigated to exclude effects of alkali binding by ASR products.

As a first step, ion balance was calculated from the Na^+, K^+, SO_4^{2-} and OH^- ion concentrations for a plausibility check of pore solution composition. For temperatures over 40 °C (Table 3, FC), ion balance has to be calculated from the equitation $[Na^+] + [K^+] \approx [OH^-] + [SO_4^{2-}]$ [24; 25]. The OH^-/SO_4^{2-} ratio reflects the chemical and thermal stability of calcium sulfoaluminate hydrates, such as ettringite. At temperatures over 40 °C, a decrease in the OH^-/SO_4^{2-} ratio was observed compared to 20 °C. As a result, the pH value of the pore solution decreases. This should reduce the solubility of the SiO_2 [26] and thus the solubility of the fly ash, which reduces pozzolanic reaction as well as solubility of the reactive aggregate and ASR product formation. On the other hand, the SiO_2 solubility increases with increasing temperature [26; 27]. The present investigations could not elucidate which one of these opposing mechanisms predominates.

Table 3 Pore solution analysis of pastes at 20 °C at different ages. FC = 9 month storage in the fog chamber at 40°C / 100% RH.

	Age [d]	Na^+	K^+	Al^{3+} mmol/l	SO_4^{2-}	OH^-
OPC	1	63	472	0.01	73	379
	28	100	575	0.05	14	677
	91	110	648	0.04	25	695
	FC	124	621	0.05	54	609
OPC-15FA	1	64	409	0.03	73	328
	28	99	495	0.06	9	594
	91	103	489	0.25	15	566
	FC	128	469	0.38	40	450

Table 3 shows the results of the concentrations of Na^+, K^+, Al^{3+}, SO_4^{2-} and OH^- ions in the pore solution of the pastes. The addition of 15 wt. % FA lowers OH^- concentration as well as the K^+ concentration due to the dilution effect. As described above, a reduction in pH reduces the SiO_2 solubility and thus the formation of ASR products. In contrast, Na^+ concentration remains nearly the same for both binders, while Al^{3+} concentration is significantly increased for the sample OPC-15FA. This indicates a contribution of the fly ash releasing notable amounts of Na^+ and Al^{3+}.

The Al^{3+} concentration of the pore solution plays an important role due to the ASR. It affects the binding of silicon in non-swellable aluminosilicates [28; 29], the formation of C-A-S-H phases [14] and the incorporation of Al in ASR gels [16]. Therefore, it is important to investigate the composition and morphology of the ASR products formed in the concretes (OPC vs. OPC-15FA) at different storage conditions.

3.3 Effect on ASR product composition and morphology

3.3.1 Polarisation microscopy

The microscopic examination showed significant ASR damage for the concrete specimens OPC stored in the fog chamber and outdoor storage after 4.5 and 9 years. This can be seen by net-like cracks in the binder matrix and aggregates in the concrete, as well as the presence of significant amounts of ASR products (Figure 4). However, the outdoor-stored concrete contained larger quantities of ASR products and increased amounts of cracks than the fog chamber-stored concrete (results not shown here). These observations are in agreement with the results from the crack width measurements (Figure 1).

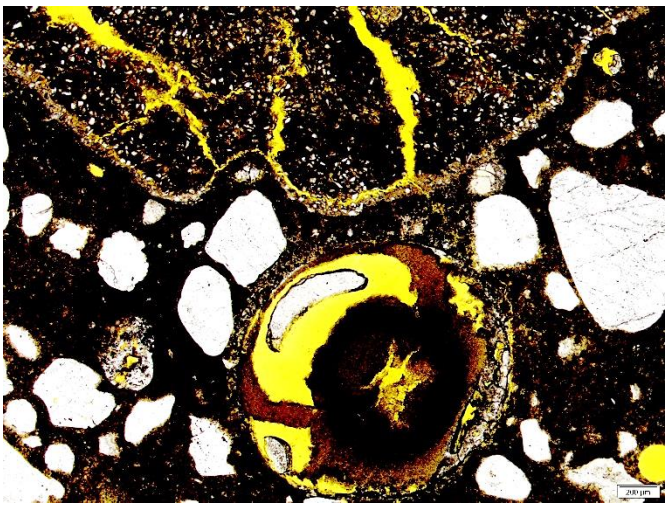

Figure 4 Microscopic image of the OPC concrete after 4.5 years in outdoor storage. Opal Sandstone grain cracked by ASR and ASR product formation in the adjacent pore.

The OPC-15FA samples show larger amounts of ettringite in air voids compared to the samples OPC in both storage conditions. The concrete sample OPC-15FA shows signs of a damaging ASR after 4.5 years and more obvious after 9 years in the outdoor storage. This can be seen by cracks in the concrete structure as well as ASR product as crack filling and in pores, detected in many places (Figure 5).

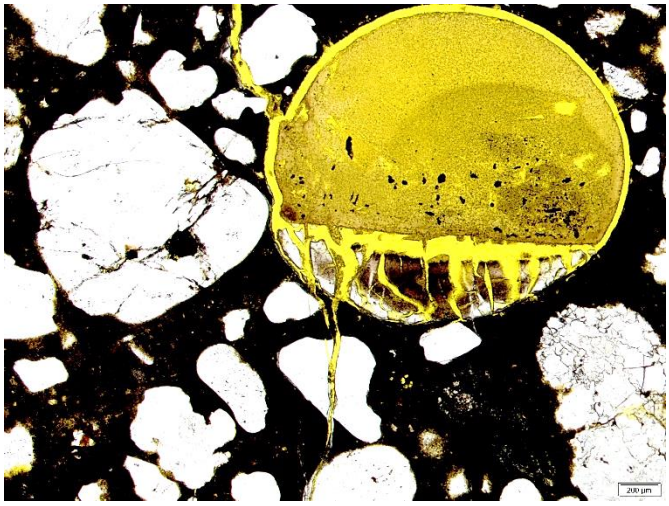

Figure 5 Microscopic image of the concrete OPC-15FA after 9 years in outdoor storage. Cracks and pores filled with ASR products. The cracks from the aggregates continue into the binder matrix.

However, the sample OPC-15FA stored in the fog chamber at 40 °C shows no signs of damaging ASR until the age of 9 years. Few cracks occur in the microstructure and rarely ASR product is found in air voids. Overall, the microstructure is intact. Thus, this sample was not considered further.

3.3.2 Scanning electron microscopy (SEM/EDX)

To investigate morphology and composition of the ASR products SEM-EDX was used. Within the scope of the study, the following questions were to be answered.

a) *Does the morphology of the outdoor exposed concretes (OPC vs. OPC-15FA) change?*
b) *Are there any differences in the composition of the ASR products formed with and without fly ash?*
c) *Is there any difference between the ASR product morphology in the OPC concrete stored outdoors or in the fog chamber?*

The SEM investigations confirmed the observations from polarized light microscopy. Damaging ASR could be detected in the OPC concrete samples both in the fog chamber and in the outdoor storage. Similar results exhibit the outdoor stored OPC-15FA sample.

15 wt.% fly ash in the binder of the concrete was not sufficient to prevent ASR after 4.5 years. ASR could only be avoided using 30 wt.% and more fly ash in the binder (results not shown here). The direct comparison of the two concretes (OPC vs. OPC-15FA) in the outdoor storage showed no difference in the morphology of the ASR products.

Nevertheless, two different ASR products could be distinguished in each ASR-damaged concrete: a crystalline and an amorphous ASR product. It could be seen that the crystalline ASR product is internally surrounded by an amorphous product (Figure 6). Similar observations were made by Leemann et al. [30], where they concluded that amorphous ASR products form first leading to cracks in the aggregate. Afterwards a crystalline product forms and fills the crack.

Crystalline ASR products can be found in air voids as well as in cracks within the aggregate grain. These crystalline products occur in both samples (OPC and OPC-15FA) stored outdoor. These observations can already be made after 4.5 years of outdoor storage.

For the formation of crystalline ASR products, certain temperatures are necessary. Leemann et al. and Shi et al. showed that large quantities of crystalline ASR products can form at temperatures around 40 °C in concrete and for artificial synthesized ASR products [5; 31]. Such temperatures can also occur on the concrete surface if it is exposed to solar radiation (especially in summer), see chapter 2.1.

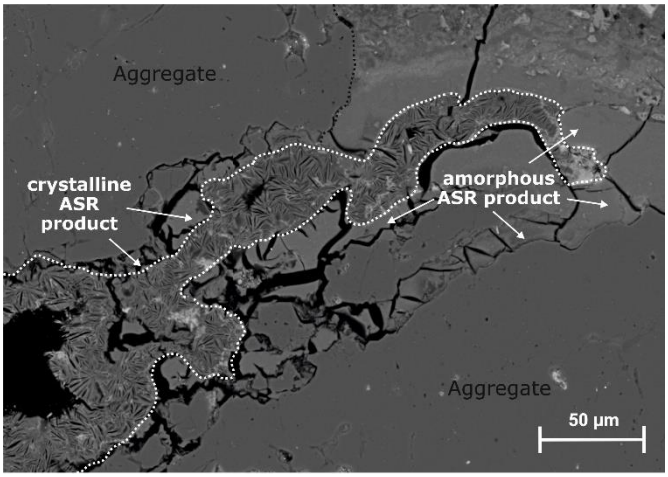

Figure 6 BSE image of concrete sample OPC after 9 years of outdoor storage shows amorphous and crystalline ASR products in a cracked aggregate. Dotted line indicate the area of the crystalline product.

Besides ASR products, ettringite can be identified in cracks after 9 years of storage (Figure 7). Ettringite occurs both in the fog chamber and in the outdoor storage. However, it is interesting to note that 15 wt.% fly ash did not prevent the formation of ettringite. Already after 4.5 years, larger amounts of ettringite could be observed in air voids. However, these did not lead to any damage in the concrete, as the formation is secondary. The increased occurrence of ettringite in air voids for the OPC-15FA concrete compared to the OPC concrete might be due to higher concentration of aluminum in the pore solution (Table 3). As these formation did not lead to any damage this will not be discussed further here.

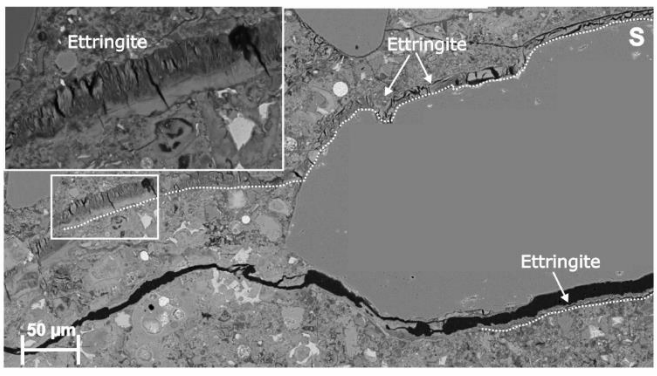

Figure 7 BSE image of concrete sample OPC-15FA after 9 years exposed to outdoor storage. Ettringite is filled in cracks.

In order to see if the composition of the formed ASR products differ they were examined in more detail.

The chemical composition of the amorphous ASR products strongly depends on the alteration by aging. Another influencing factor is the chemical environment during gel formation (in aggregate or in cement matrix). In the case of close contact to the hardened cement paste matrix, an increase in the Ca content can be expected as well as with increasing age and increasing distance from the reactive aggregate [6; 32].

In the literature, the composition of crystalline ASR products found in concrete are described as quite homogeneous. Ratios of Ca/Si = 0.23- 0.35 and (Na+K)/Si = 0.22 - 0.33 are mentioned [31]. The situation is different for the amorphous ASR products in concretes, where greater differences in composition (Ca/Si = 0.2 - 0.6, (Na+K)/Si = 0.2 - 0.7) are reported [30; 31].

The SEM studies showed that crystalline ASR products formed already after 4.5 years in the outdoor storage (Figure 8 a)). The Ca-heatmap for the OPC concrete reveal a Ca concentration around 10-14 wt.% for the formed ASR products (Figure 8 b)). There was no difference in the Ca-heatmap between the crystalline and amorphous ASR products observed, which means that the composition of Ca is the same. This is in accordance with the observations of Leemann et al. [31]. They reported only slight differences in the Ca content for amorphous and crystalline ASR products.

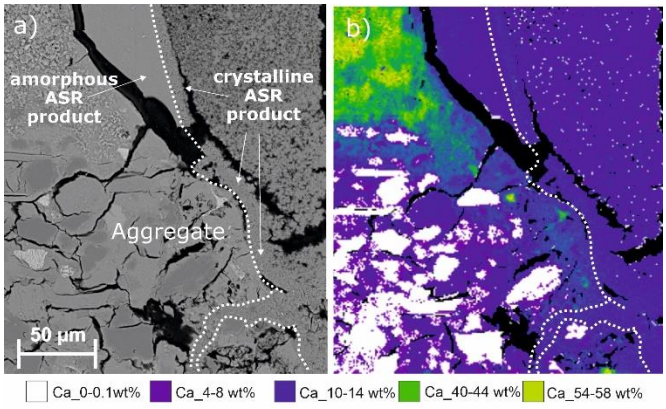

Figure 8 Images of the OPC concrete after 4.5 years in outdoor storage. ASR products filled in a crack in an aggregate and in air void. Dotted line indicates the boundary of the crystalline and the amorphous product. a) BSE image b) Ca-heatmap.

However, Leemann et al. [31] reported greater differences in the (Na+K)/Si ratios between the crystalline and amorphous products. Figure 9 a) shows a BSE image of amorphous and crystalline products in an air void for the 100 wt.% OPC concrete. The ASR products appear as a rim inside of the air void. Although the morphology differs no differences in the composition could be detected. The K-heatmap shows no significant concentration differences between the ASR products (Figure 9 b)). The Ca/Si and K/Si ratios of the ASR products in direct contact are similar. The averaged ratios for the ASR products here were 0.22 for Ca/Si and 0.26 for K/Si.

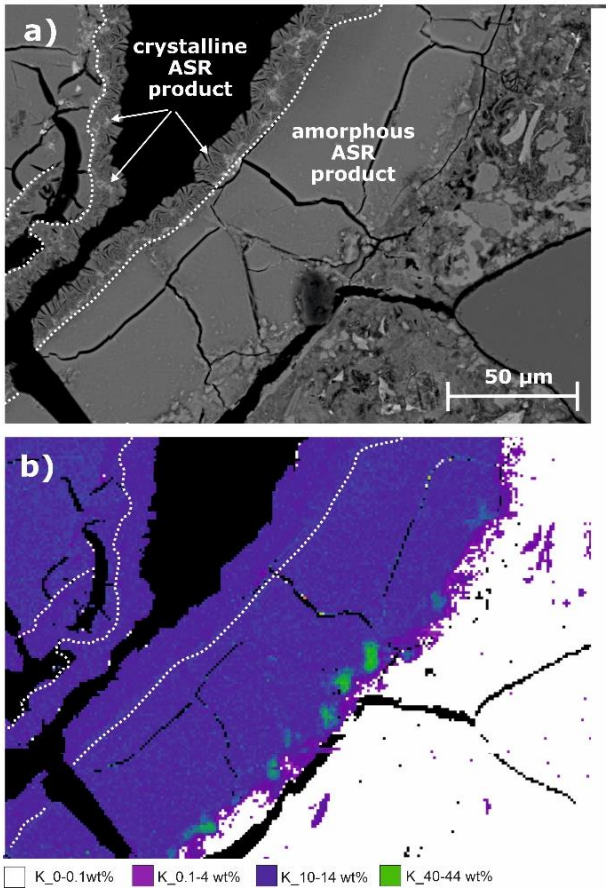

Figure 9 Images of the OPC concrete after 9 years in outdoor storage. a) BSE Image of amorphous and crystalline ASR products in an air void. b) K-heatmap. Dotted line indicates the boundary of the crystalline and the amorphous product.

As only very low concentrations, below the detection limit, of Na are present in the ASR products, the element was neglected for the evaluation of the compositions. In Figure 10 the ternary diagram shows the compositions (Ca, Si and K) for the ASR products in the respective concretes (OPC and OPC-15FA) after 9 years in the outdoor storage. The measurement points were determined both inside the aggregate grain, at crack fillings in the cement paste matrix, and in air voids.

Investigations by Dressler [9] and Krüger et al. [18] have shown that the use of Al-rich SCMs can alter the composition of ASR gels. Krüger et al. showed that Al can be incorporated into the structure of synthetic ASR gels [16]. However, investigations by Shi et al. have shown that for crystalline products no incorporation of Al is possible. The presence of Al has even led to destabilization of the ASR product [33].

In the present study, no Al was detected in the ASR products in the concrete samples, not even in the sample with 15 wt.% fly ash. One reason for this could be that although the fly ash provides more Al (Table 3) than the pure Portland cement, Al is preferentially incorporated in C-(A)-S-H phases [10; 14; 15]. In addition, Al could be required for the secondary formation of ettringite.

The ternary diagram data plot shows, that on average, the compositions of the ASR products formed in the concretes OPC and OPC-15FA are the same. The average molar ra-

tios were 0.32 for Ca/Si and 0.22 for K/Si. This composition corresponds to the average composition given by Leemann et al. for crystalline ASR products [31].

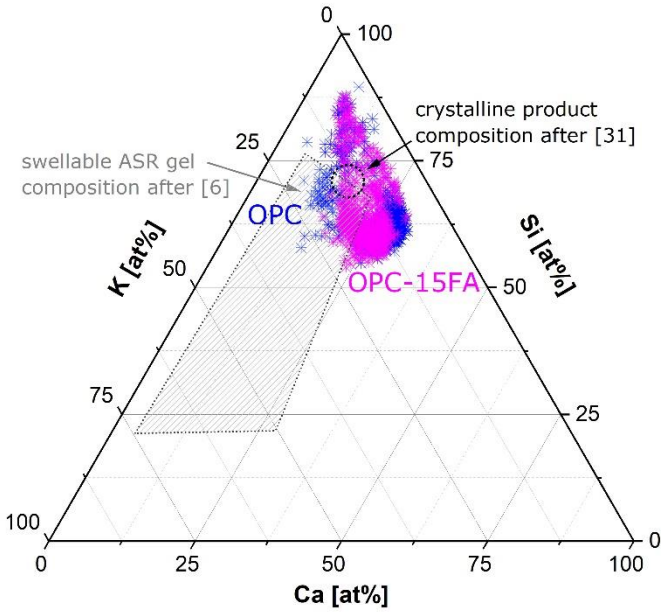

Figure 10 Ternary diagram of the SEM/EDX results for the OPC and OPC-15FA concrete after 9 years in the outdoor storage. The point clouds represent the composition of each measured pixel point for the ASR products (blue: OPC, pink: OPC-15FA). The dashed circle represent the typical crystalline product composition [31]. The dashed rectangle represents the composition range for swellable ASR gels [6].

For the OPC sample, Ca/Si ratios of 0.08-0.51 and K/Si ratios of 0.06-0.44 could be determined. For the OPC-15FA sample the ratios were in the range of 0.07-0.51 for Ca/Si and in the range of 0.06-0.41 for K/Si. The direct comparison of the compositions for the tested concrete samples shows no change in ASR product composition due to the use of 15 wt.% fly ash. The areas for high Ca/Si ratios correspond to the ASR products that had formed in direct contact with the hardened cement paste. These are the compositions that Mansfeld classified as non-damaging [6]. In areas with less calcium (e.g. in the aggregates), more swellable ASR gels are present.

The investigations with polarized light microscopy and UV incident light microscopy have shown the occurrence of damaging ASR for the concrete mixes OPC stored outdoors and in the fog chamber. However, larger amounts of ASR products are present in the concretes in the outdoor storage (chapter 3.3.1).

For the OPC-15FA concrete, larger discrepancies between the storage conditions could be found, since even after 9 years no damaging ASR occurred in the fog chamber, but in the outdoor storage. This is in correlation with the measured crack widths, as the concrete stored in the fog chamber showed maximum crack widths of 0.15 mm (Figure 2). Since, no larger amounts of ASR products could be detected in the OPC-15FA concrete, this sample was not investigated further.

Figure 11 a) shows a BSE image of the concrete after 9 years in the fog chamber. Within the concrete structure mainly ASR but some areas of secondary formed ettringite could be observed like in the outdoor stored concretes.

Figure 11 b) shows the Ca-heatmap of the OPC sample after 9 years storage in the fog chamber. Strong signs of leaching and carbonation could be observed, which is why no closer characterization of the composition of the ASR products was possible here. The direct comparison of the ASR products formed under different storage conditions (fog chamber vs. outdoor storage) showed differences in the morphology. The ASR product formed in the fog chamber concrete did not show platy or rosette-like surfaces structures, which were observed in the products, formed outdoors. Additionally, clear boundaries between amorphous and crystalline ASR products, as described in Figure 6 for samples stored outdoors, could not be observed in the concrete stored in the fog chamber.

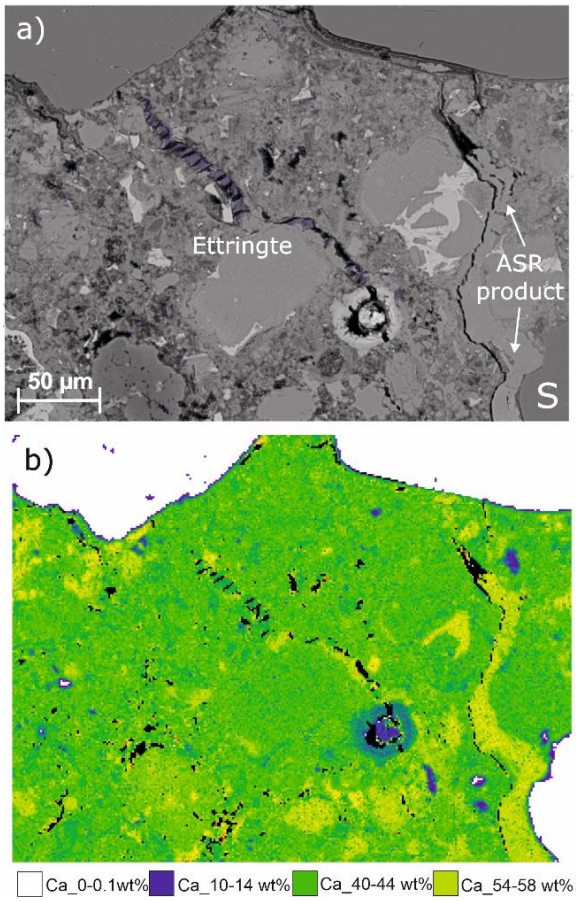

Figure 11 Images of the concrete OPC after 9 years storage in the fog chamber at 40°C. a) BSE image shows ettringite (purple areas for S) and ASR product as crack filling. B) Ca-heatmap shows fully carbonation of the former ASR product.

Similar observations were made by Leemann et al. [34]. They could observe differences in the morphology but not in composition of the ASR products exposed in laboratory or field exposed concrete. Their results show that the storage conditions have an effect on the morphology of ASR products, but not necessarily on their composition and thus on their swelling capacity.

4 Conclusion

Concretes cubes with 100 wt.% OPC (OPC) as well as 75 wt.% OPC and 15 wt.% fly ash (OPC-15FA) were stored outdoors at Munich climate and in a fog chamber at 40°C/100% RH for up to 9 years and were investigated with respect to their cracking behavior, porosity, pore so-

lution composition and ASR products distribution, morphology and composition. The following conclusions can be drawn:

- As expected, the crack width analysis showed that significantly larger crack widths occurred for the concretes OPC stored outdoors than in the fog chamber. This can be explained by higher quantities of ASR products and additionally effects, e.g. freeze-thawing in the winter period, for which the ASR induced cracks are precursors.

- When stored in the fog chamber, sample OPC-15FA did not show clear signs damaging ASR. However, same samples exposed to natural outdoor weathering in Munich did. Porosity measurements showed a densification of the capillary pores due to an acceleration of the pozzolanic reaction in the fly ash concrete exposed to enhanced temperatures. This may lead to an overestimation of the concrete assessment during the fog chamber storage.

- Pore solution analysis indicates lower OH^- concentrations in fly ash pastes at 20 °C as well as at 40 °C, which entails lower SiO_2 solubility of reactive aggregates but also of the pozzolanic reaction. The present investigations could not elucidate which one of these opposing mechanisms predominates. Nevertheless, Na^+ and Al^{3+} is also released into the pore solution by the fly ash.

- The examination of the concretes by SEM/EDX showed no indication of significant differences in the morphology of the concretes OPC or OPC-15FA at outdoor storage. In the concrete samples, two ASR products (crystalline and amorphous) could be classified, which did not show major compositional differences in direct contact, but could be distinguished by morphological properties.

- The molar ratios of the ASR products found were in the range of 0.1-0.5 for Ca/Si and in the range of 0.1-0.4 for K/Si. The bulk composition of these products was Ca/Si = 0.3 and K/Si = 0.2, which is in the range of swellable ASR gels composition.

- The comparison of the concrete storage condition (outdoor and fog chamber) showed differences in the morphology of the ASR products. The structure of the ASR products formed in the fog chamber showed no platy or rosette-like surfaces structures unlike those formed during outdoor storage. No clear boundaries between amorphous and crystalline products could be observed here.

The present investigations show that accelerated test methods consider only partial aspects of the complex mechanisms of an ASR in concretes containing fly ash. For concretes with pure OPC accelerated concrete tests by fog chamber storage show similar results due to ASR as it occurs under natural weathering. Storage conditions have a direct effect on the quantities and morphology of the ASR products, the porosity and the pore solution composition of the concrete samples. When testing binders with a more complex composition, opposing mechanisms are achieved and the chemical and physical processes can be changed significantly by accelerating conditions.

Acknowledgments

The authors would like to thank the German Research Foundation (project number: 438217913) for their financial support. We are grateful for the help of Kai Fischer for the production of the concrete specimens and the pre-evaluation of the data. We would like to thank the mineralogical laboratories of the Centre for Building Materials (cbm) at the Technical University of Munich for their assistance in the project. We would like to thank Stefanie Lode from NTNU for the SEM-AM measurements and helpful discussion. The Research Council of Norway is acknowledged for the support to the Norwegian Laboratory for Mineral and Materials Characterisation, MiMaC, project number 269842/F50.

References

[1] Deutscher Ausschuss für Stahlbeton: Vorbeugende Maßnahmen gegen schädigende Alkalireaktion im Beton (Alkali-Richtlinie), Oktober 2013.

[2] Stark, J.; Wicht, B. (2013) *Dauerhaftigkeit von Beton*. 2. Aufl. Berlin Heidelberg: Springer.

[3] Lindgård, J. et al. (2012) *Alkali–silica reactions (ASR): Literature review on parameters influencing laboratory performance testing* in: Cement and Concrete Research 42, v. 2, p. 223–243. https://doi.org/10.1016/j.cemconres.2011.10.004

[4] Shi, Z. et al. (2019) *Synthesis, characterization, and water uptake property of alkali-silica reaction products* in: Cement and Concrete Research 121, p. 58–71. https://doi.org/10.1016/j.cemconres.2019.04.009

[5] Shi, Z. et al. (2020) *Synthesis of alkali-silica reaction product structurally identical to that formed in field concrete* in: Materials & Design 190, p. 108562. https://doi.org/10.1016/j.matdes.2020.108562

[6] Mansfeld, T. (2008) *The swelling behaviour of alkali silicate gels considering their composition* [Doctoral dissertation]. Bauhaus-Universität Weimar.

[7] Wieker, W.; Hübert, C.; Heidemann, D.; Ebert, R. *Zur Reaktion von Alkaliverbindungen mit Kieselsäure und Silicaten im Hinblick auf betonschädigende Dehnungsreaktionen* – 14. Internationale Baustofftagung - Ibausil, Weimar, p. 1-0911 - 1-0929, 2000.

[8] Dent Glasser, L. S. (1979) *Osmotic pressure and the swelling of gels* in: Cement and Concrete Research 9, v. 4, p. 515–517.

[9] Dressler, A. (2013) *Effect of de-icing salt and pozzolanic, aluminous supplementary cementitious materials on the mechanisms of damaging alkali-silica reaction in concrete* [Doctoral dissertation]. Technische Universität München.

[10] Ramlochan, T.; Thomas, M.; Hooton, R. (2004) *The effect of pozzolans and slag on the expansion of mortars cured at elevated temperature* in: Cement and Concrete Research 34, v. 8, p. 1341–1356. https://doi.org/10.1016/j.cemconres.2003.12.026

[11] Wild, S.; Khatib, J. M.; Jones, A. (1996) *Relative strength, pozzolanic activity and cement hydration in superplasticised metakaolin concrete* in: Cement and Concrete Research 26, v. 10, p. 1537–1544.

[12] J. A. Kostuch, V. Walters, T. R. Jones (1993) *High performance concretes incorporating metakaolin: a review* in: Concrete, v. 2, p. 1799–1811.

[13] Sabir, B. B.; Wild, S.; Bai, J. (2001) *Metakaolin and calcined clays as pozzolans for concrete: a review* in: Cement and Concrete Composites 23, p. 441–454.

[14] Schäfer, E. (2004) *Einfluss der Reaktionen verschiedener Zementhauptbestandteile auf den Alkalihaushalt der Porenlösung des Zementsteins* [Doctoral dissertation]. Technischen Universität Clausthal.

[15] Medhat H. Shehata; Michael D.A. Thomas; Roland F. Bleszynski (1999) *The effects of fly ash composition on the chemistry of pore solution in hydrated cement pastes* in: Cement and Concrete Research 29, v. 12, p. 1915–1920. https://doi.org/10.1016/S0008-8846(99)00190-8

[16] Krüger, M. E.; Heisig, A.; Hilbig, H.; Eickhoff, H.; Heinz, D (2023) *Effect of Aluminum on the Structure of Synthetic Alkali-Silica Gels* in: Cement and Concrete Research, v. 166, 107088. https://doi.org/10.1016/j.cemconres.2022.107088

[17] DIN EN 450-1 – *Flugasche für Beton – Teil 1: Definition, Anforderungen und Konformitätskriterien*; Deutsche Fassung EN 450-1:2012, Oktober 2012.

[18] Krüger, M. E.; Woydich, E.; Weerdt, K. de; Heisig, A.; Machner, A. *Can the R³-test be used as a rapid screening test for the ASR mitigation potential of calcined clays?* - Calcined Clays for Sustainable Concrete, Lausanne, Switzerland, 2022.

[19] Geiger, R. Classification of climates after W. Köppen – Landolt-Börnstein – *Zahlenwerte und Funktionen aus Physik, Chemie, Astronomie, Geophysik und Technik, alte Serie.* Berlin: Springer. v. 3. p. 603–607.

[20] Lugauer, M. (2015) *Witterungsverhältnisse, Münchner Statistik*, 3. Quartalsheft, Statistisches Amt der Landeshauptstadt München, p.1-5.

[21] Peyerl, M.; Krispel, S.; Weihs, P.; Maier, G. (2016) *Stadtverkehrsflächen – Optimierter Beton für den innerstädtischen Bereich*, Bericht update 44.

[22] Heiles, B. (2022) *Witterungsverhältnisse*, Münchner Statistik, 1. Quartalsheft, Statistisches Amt der Landeshauptstadt München, p. 40-47.

[23] https://de.climate-data.org (accessed 19.04.2023).

[24] Schmidt, K. (2009) *Avoiding a damaging alkali silica reaction with fly ash* [Doctoral dissertation]. Technische Universität München.

[25] Schmidt, K.; Urbonas, L.; Dressler, A.; Heinz, D. (2009) *AKR Performance-Prüfung von flugaschehaltigen Betonen - Einfluss der Temperatur auf die Porenlösung und Möglichkeiten zur zielsicheren Bewertung*, 17. internationale Baustofftagung - ibausil, Weimar, p. 2-0267 – 2-0276, 2009.

[26] Iler, R.K. (1973) *Effect of adsorbed alumina on the solubility of amorphous silica in water in: Journal of colloid and interface science* 43, v. 2, p. 399–408. https://doi.org/10.1016/0021-9797(73)90386-X

[27] Berninger, A. M. (2005) *Mikrostrukturelle Eigenschaften von Quarz als Bestandteil spät reagierender, alkaliempfindlicher Zuschläge* [Doctoral dissertation]. Bauhaus-Universität Weimar.

[28] Hünger, K.-J. (2007) *The contribution of quartz and the role of aluminum for understanding the AAR with greywacke* in: Cement and Concrete Research 37, v. 8, p. 1193–1205.

[29] Hill, S. (2004) *Zur direkten Beurteilung der Alkaliempfindlichkeit präkambrischer Grauwacken aus der Lausitz anhand deren Kieselsäure- und Aluminiumlöseverhalten* [Doctoral dissertation]. TU Cottbus.

[30] Leemann, A. (2017) *Raman microscopy of alkali-silica reaction (ASR) products formed in concrete* in: Cement and Concrete Research, v. 102, p. 41–47. https://doi.org/10.1016/j.cemconres.2017.08.014

[31] Leemann, A.; Shi, Z.; Lindgård, J. (2020) *Characterization of amorphous and crystalline ASR products formed in concrete aggregates* in: Cement and Concrete Research 137, 106190. https://doi.org/10.1016/j.cemconres.2020.106190

[32] Knudsen, T.; Thaulow, N. (1975) *Quantitative microanalyses of alkali-silica gel in concrete* in: Cement and Concrete Research 5, v. 5, p. 443–454. https://doi.org/10.1016/0008-8846(75)90019-8

[33] Shi, Z.; Ma, B.; Lothenbach, B. (2021) *Effect of Al on the formation and structure of alkali-silica reaction products* in: Cement and Concrete Research 140, 106311. https://doi.org/10.1016/j.cemconres.2020.106311

[34] Leemann, A.; Borchers, I.; Shakoorioskooie, M.; Griffa, M.; Müller, C.; Lura, P. (2019) *Microstructural analysis of ASR in concrete - accelerated testing versus natural exposure* – International Conference on Sustainable Materials, Systems, Rovinj, Croatia.